Supplementary Materials for

Remarkable regression of diffuse coronary atherosclerosis in patients with triglyceride deposit cardiomyovasculopathy

Ken-ichi Hirano*, Masahiro Higashi, and Kenichi Nakajima

*Correspondence to: khirano@cnt-osaka.com

This PDF file includes:

Methods

Diagnosis of TGCV

The diagnosis was made according to the diagnostic criteria of TGCV, developed by our study group (1). The present patients fulfilled the requirements for definite diagnosis of TGCV: the marked reduction of myocardial washout rate (WR) of iodine-123-β-methyl-p-iodophenyl-pentadecanoic acid (BMIPP) and the diffuse coronary atherosclerosis as essential and major items, respectively.

Dietary tricaprin intake and ethical approval

Cases 1 and 2 added tricaprin to their usual diets using commercially available food supplements. Tricaprin is a class of medium-chain triglycerides (MCT). Synthetic MCT have been used in daily clinical practice for 60 years worldwide for patients with metabolic, cardiovascular, and neurological disorders (2, 3). In Japan, several kinds of food products (oil, powder, and jelly), with variable tricaprin composition, have been available during the last couple of decades (4, 5). The selection of food products was supervised by dieticians and physicians. In cases 1 and 2, the amount of tricaprin taken was calculated to be approximately 1.5g/day and 4.5g/day, respectively, much smaller than that used for ketogenic diets in patients with cancer or neurological disorders (2, 5). Patients were instructed to continue other medical therapies. No adverse effects were reported. A TGCV patient group (http://tgcv-pt-group.com/) supported patients when required. Information from the clinical charts, imaging, and laboratory data was collected after the patient completed an informed consent form. This study was approved by the Osaka University Hospital Ethical Committee (Approved No. 14207), and written informed consent was obtained from the patients.

Image processing of coronary computed tomography angiography (CTA) with a color-coded display

Coronary CTA was performed by the standard protocol of Osaka University Hospital, including pre-treatment by sublingual administration of 0.6 mg of nitroglycerin. The obtained anonymous data was transferred to an independent expert in diagnostic radiology, then analyzed as described below. The rationale behind the color-coded display is that tissue triglyceride (TG) contents are closely correlated to the CT number in Hounsfield units (HU) (6). Therefore, the low-attenuation area and its coronary arterial wall volume indicate the lipid distribution and content.

The coronary artery-related data were segmented manually by the expert radiologist based on CT images acquired at a resolution of 0.39×0.39×0.63 mm, and subsequent image processing was implemented using MeVisLab (Mevix Medical Solution, AG. Bremen Germany, http://mevislab.de). For more precise detection of vascular wall components, the original image was resized to 0.1×0.1×.0.1 mm without changing the image spectrum. These resized images were segmented by setting four calibrated intensity (HU) thresholds: -25–0 yellow; 0–40, orange; 40–215, green; 215–700, white). Smoothing was deemed necessary before further steps to remove noise, with crucial shape feature preservation. Each centerline was generated by the distance-map method along with the coronary arteries for the positioning of their cross-sections. Subsequently, a sequence of color-labeled arterial cross-sections was obtained. In the coronary arteries obtained from patients with TGCV, abundant low-attenuation areas (yellow and orange) indicating lipid deposition were observed within the arterial wall. These areas were predominantly distributed on the adventitial side and protruded from the outside towards the inside in a nodular, peninsular, or bridging pattern; this was different from the distribution observed in non-TGCV coronary arteries, as reported elsewhere (7–9).

Volume calculation of coronary artery wall with lipid and lumen

To quantify the volume of coronary artery wall with diffuse lipid involvement, we used the VINCENT coronary artery analysis application (Fujifilm Medical Co., Ltd., Tokyo, Japan), as shown in Fig. S3. On the automatically created curved planar reconstruction, the coronary arteries were divided according to the CT value (low-attenuation wall: -25≤ HU<40; high attenuation wall: 40≤ HU<215; lumen: 215≤ HU<700; calcification: 700≤ HU). Each volume was calculated. Percentage changes of volumes with each HU range between measurements before and after treatments with tricaprin were calculated and shown in the middle of panel B. The measurement range included the right coronary artery #1–3, left main trunk-left anterior descending artery #5–7, and left circumflex artery #11, #13; the segment where the stent was placed was excluded.

Evaluation of myocardial lipolysis of TG with ^{123}I-β-methyl-p-iodophenyl-pentadecanoic acid (^{123}I-BMIPP) in scintigraphy

^{123}I-BMIPP is a radioactive long-chain fatty acid (LCFA) (10). In Japan, since 1993, this tracer has been approved by the Ministry of Health, Labour, and Welfare, as an *in vivo* radiotracer for evaluating myocardial LCFA and TG metabolism in heart diseases. Through the first pass, ^{123}I-BMIPP is immediately taken up; most of it is incorporated into the TG pool, and then hydrolyzed and degraded in cardiomyocytes (11). Because it reflects myocardial lipolysis (12), the washout rate (WR) of ^{123}I-BMIPP is an essential item within the diagnostic criteria for TGCV (1).
In both patients, BMIPP scintigraphy was performed after overnight fasting. Only water intake was allowed by the timing of delayed images to minimize the potential effects of food intake and changes in serum glucose or fatty acid levels on the uptake and WR of BMIPP. Following the

protocol recommended by the Japanese Society of Nuclear Cardiology, after fasting for ≥12 h, 111 MBq of ^{123}I-BMIPP (Cardiodine; Nihon Medi-Physics Co. Ltd., Tokyo, Japan) was intravenously injected at rest. Early and delayed images were obtained after 20 minutes and between 180 and 210 minutes, respectively (13). For each patient, the allowance for the differences in the time interval between the early and delayed images was within ± 5 min. The obtained anonymous data was transferred to an independent expert in nuclear cardiology, then analyzed as briefly described below (14).

Short-axis SPECT data were imported in DICOM format and slices that did not include the myocardium were excluded. Early and delayed DICOM images were imported to create short-axis images and adjusted for the time-decay correction. The most apical and basal slices that included extracardiac activity were excluded; that is, only ring-shaped slices were selected to avoid partial volume effects at both ends. The average counts on the early and delayed short-axis image were used for calculating WRs.

The WR (%) was calculated as:

$$\frac{\text{Early cardiac counts} - \text{Delayed cardiac counts}}{\text{Early cardiac counts}} \times 100$$

The reproducibility of WR was within ± 1.5% (SD) (14). The display scale of the delayed images was time decay-corrected and adjusted to the maximum count of the early image.

Detailed case presentation

Both cases had suffered from refractory angina pectoris and coronary artery disease. However, the diagnosis of TGCV was an apparent clinical turning point as described below.

Case 1 (Panel A) was that of a 65-year-old man (BMI=29.1) presenting with anterior chest pain occurring mainly at night, which had started a couple of months before. He visited different hospitals; however, he remained undiagnosed. He developed cerebral infarction due to the stenosis of the left middle cerebral artery and visited the neurological department of our institute, which referred him to the cardiology department for chest pain. Clinical history included type 2 diabetes mellitus (DM), dyslipidemia, and hypertension. No evidence of diabetic nephropathy or retinopathy was reported. The coronary CTA showed diffuse atherosclerosis in the mid-portion of the left anterior descending branch. The indication of percutaneous coronary intervention (PCI) was excluded. His chain pain with ST-segment depression in the Holter electrocardiography often required a high dose (5 tablets) of nitroglycerine for relief. Medical therapy was started and included beta-blockers, calcium antagonists, and nitrates. His dyslipidemia and DM were properly treated by administrating rosuvastatin, glimepiride, sitagliptin, and metformin during the clinical course (please see Table S1). Because his chest pain was unsuccessfully treated with nitrate, diltiazem, amlodipine, and bisoprolol, a further examination of the diagnosis for TGCV was needed. He met the criteria because of the marked reduction in WR of BMIPP and diffuse coronary atherosclerosis. Diagnosis of TGCV was made. This patient started the dietary therapy with tricaprin-rich products and his symptoms began to relieve at around ten days and diminished three months later. WR of BMIPP was improved to 24.8% (Lower, panel A). Data from his coronary CT angiography were subjected to the CT-

based color-coded display of arterial walls we developed. As shown in middle, panel A and Fig.S1, the luminal diameter of the mid-portion of the left anterior descending artery increased. Before therapy, an abundant TG deposition was observed as orange/yellow areas within his coronary arterial walls, mainly distributing in the adventitial site and protruding from outside to inside. These patterns were markedly improved in the images dated four years after the therapy (middle, panel A). Six years after starting tricaprin, he has been free from angina.

Case 2 (Panel B) was that of a 60-year-old man (BMI=23.8) referred to our institute for the detailed examination of refractory CAD. He had a 3-year history of type 2 diabetes without nephropathy or retinopathy. Medical history included dyslipidemia and hypertension. Two years before presentation, he had acute coronary syndrome with the first onset of effort angina and received PCI at the right coronary artery with a drug-eluting stent (DES) (Ultimaster, Terumo, at #1-2). Nine months later, effort angina re-developed and another PCI with DES at #6 and 8 was performed. One year later, he visited the same hospital due to unstable angina, where he received another stent implantation and drug-coated balloon angioplasty for the in-stent restenosis of the stent placed at #6 before. Since the first admission, serum lipids, blood pressure, and glucose levels were strictly controlled (please see Table S1) with bisoprolol, azilsartan, amlodipine, rosuvastatin, ezetimibe, dapagliflozin, teneligliptin hydrobromide, aspirin, and prasugrel. We diagnosed him with TGCV with low WR of BMIPP and diffuse coronary atherosclerosis. Three months following tricaprin, regression and revascularisation were observed, quantification of coronary lipid volume was reduced, and vascular lumen volume increased (upper and middle panel B). The color-coded display showed luminal dilatation and elimination of lipid involvement from the adventitia (Fig. S2). Levels of serum lipids and HbA1c did not change

before and after tricaprin therapy (Table S1). BMIPP scintigraphy showed improved WR after tricaprin therapy, as shown in the lower panel B.

References

1. Nakajima K. Triglyceride deposit cardiomyovasculopathy: how to recognise a new disease entity. *Heart* 2021;107:93–5. doi: https://doi.org/10.1136/heartjnl-2020-318055

2. Augustin K, Khabbush A, Williams S, Eaton S, Orford M, Cross JH, et al. Mechanism of action for the medium chain triglyceride ketogenic diet in neurological and metabolic disorders. *Lancet Neurol* 2018;17:84–93. doi: https://doi.org/10.1016/S1474-4422(17)30408-8

3. Labarthe F, Gélinas R, Rosiers CD. Medium-chain acids as metabolic therapy in cardiac disease. *Cardiovasc Drugs Ther* 2008;22:97–106. doi: https://doi.org/10.1007/s10557-008-6084-0.

4. Aoyama T, Nosaka N, Kasai M. Research on the nutritional characteristics of medium-chain fatty acid. *J Med Invest* 2007;54:385–8. doi: https://doi.org/10.2152/jmi.54.385

5. Hagihara K, Kajimoto K, Osaga S, Nagai N, Shimosegawa E, Nakata H, et al. Promising effect of a new ketogenic diet regimen in patients with advanced cancer. *Nutrients* 2020;12:1473. doi: https://doi.org/10.3390/nu12051473

6. Shores NJ, Link K, Fernandez A, et al. Non-contrasted computed tomography for the accurate measurement of liver steatosis in obese patients. *Dig Dis Sci* 2011;56:2145–51. doi: 10.1007/s10620-011-1602-5.

7. Higashi M, Ikeda Y, Miyauchi H, et al. Imaging modalities for triglyceride deposit cardiomyovasculopathy. *Ann Nucl Cardiol* 2017;3:94–102. doi: https://doi.org/10.17996/anc.17-00028.

8. Li M, Hirano K, Ikeda Y. et al. Triglyceride deposit cardiomyovasculopathy: a rare cardiovascular disorder. *Orphanet J Rare Dis* 2019;14:134. doi: https://doi.org/10.1186/s13023-019-1087-4

9. Kozawa J, Higashi M, Shimomura I, Hirano K. Intractable coronary artery disease in a patient with type 2 diabetes presenting triglyceride deposit cardiomyovasculopathy. *Diabetes Care* 2019;42:983–6. doi: 10.2337/dc18-2365.

10. Knapp FF Jr, Ambrose KR, Goodman MN. New radioiodinated methyl-branched fatty acids for cardiac studies. *Eur J Nucl Med* 1986;12:S39–S44. doi: 10.1007/BF00258103

11. Fujibayashi Y, Nohara R, Hosokawa R, et al. Metabolism and kinetics of iodine-123-BMIPP in canine myocardium. *J Nucl Med* 1996;37:757–61.

12. Hirano K, Ikeda Y, Sugimura K, Sakata Y. Cardiomyocyte steatosis and defective washout of iodine-123-β-methyl iodophenyl-pentadecanoic acid in genetic deficiency of adipose triglyceride lipase. *Eur Heart J* 2015;36:875. doi: 10.1093/eurheartj/ehu417

13. Miyauchi H, Hirano K, Nakano Y, Shimada K, Nishikawa M, Yamamoto H, et al. 123I-BMIPP scintigraphy shows that CNT-01 (tricaprin) improves myocardial lipolysis in patients with idiopathic triglyceride deposit cardiomyovasculopathy: First randomized controlled, exploratoty trial for TGCV. *Ann Nucl Cardiol*. 2022;8:67–75.

14. Chen Z, Nakajima K, Hirano K, Kamiya T, Yoshida S, Saito S et al. Methods of calculating 123I-beta-methyl-P-idophenyl-pentadecanoic acid washout rates in triglyceride deposit cardiomyovasculopathy. *Ann Nucl Med*. 2022;36:986-997. https://doi.org/10.1007/s12149-022-01787-9. Online ahead of print.

Table S1

Serum lipids and HbA1c levels before and after the dietary therapy with tricaprin

	Case 1		Case 2	
	Before (n=3)	After (on treatment) (n=4)	Before (n=3)	After (on treatment) (n=3)
LDL-C (mmol/L)	2.68±0.48	2.59±0.38	1.34±0.07	1.34±0.05
HDL-C (mmol/L)	0.95±0.08	0.92±0.1	0.95±0.08	0.92±0.03
TG (mmol/L)	2.94±0.95	3.89±1.36	0.88±0.02	0.85±0.13
HbA1c (%)	7.3±0.38	7.2±0.54	7.1±0.1	7.2±0.1

All values are expressed as mean±SD.

Each number represents an independent analysis of blood drawn on different dates of the same patients.

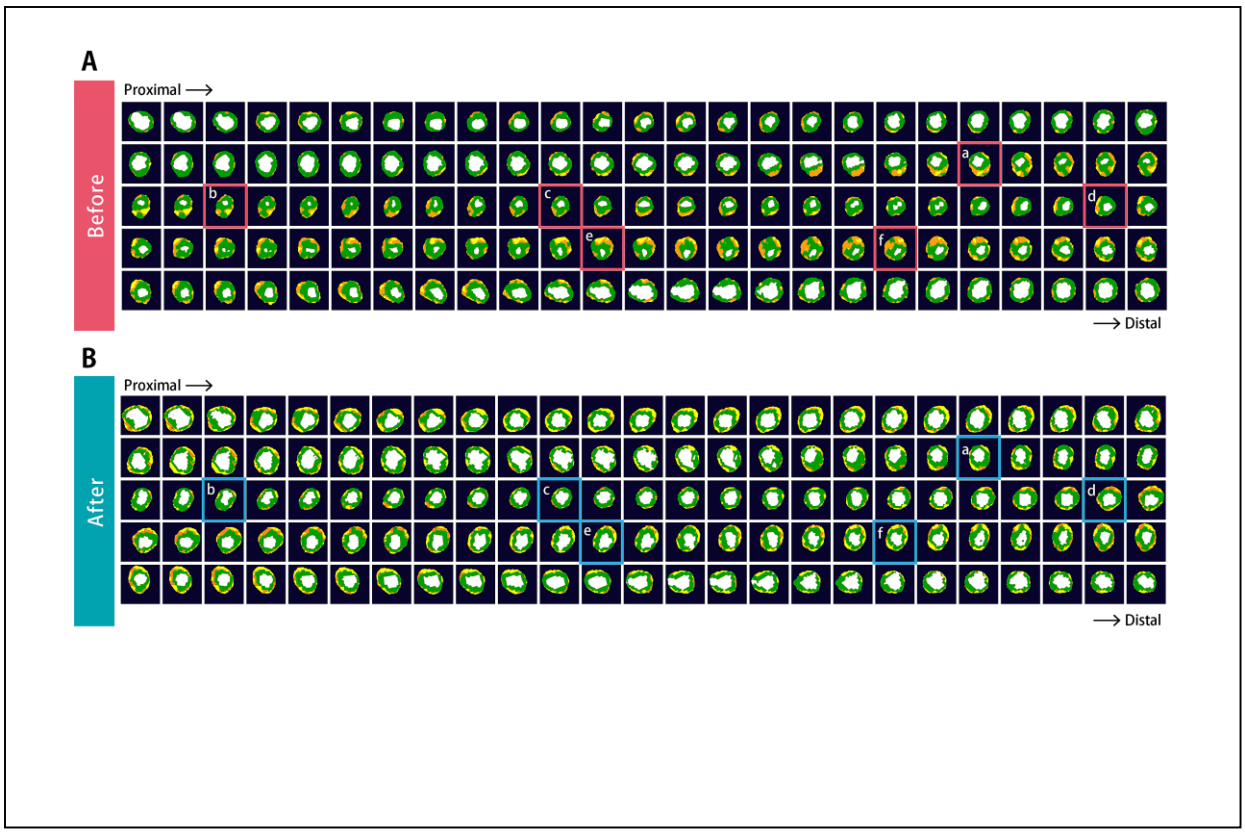

Fig. S1. Supplementary coronary CT images with a colour-coded display in case 1 (panel A)

The color-coded short-axis CT images before (**A**) and after (on-treatment) (**B**) tricaprin treatment. The short-axis images of the left coronary anterior descending artery are shown at every 0.2 mm: a, b, c, d, e, and f correspond to the cross-sectional images in the middle panel A.

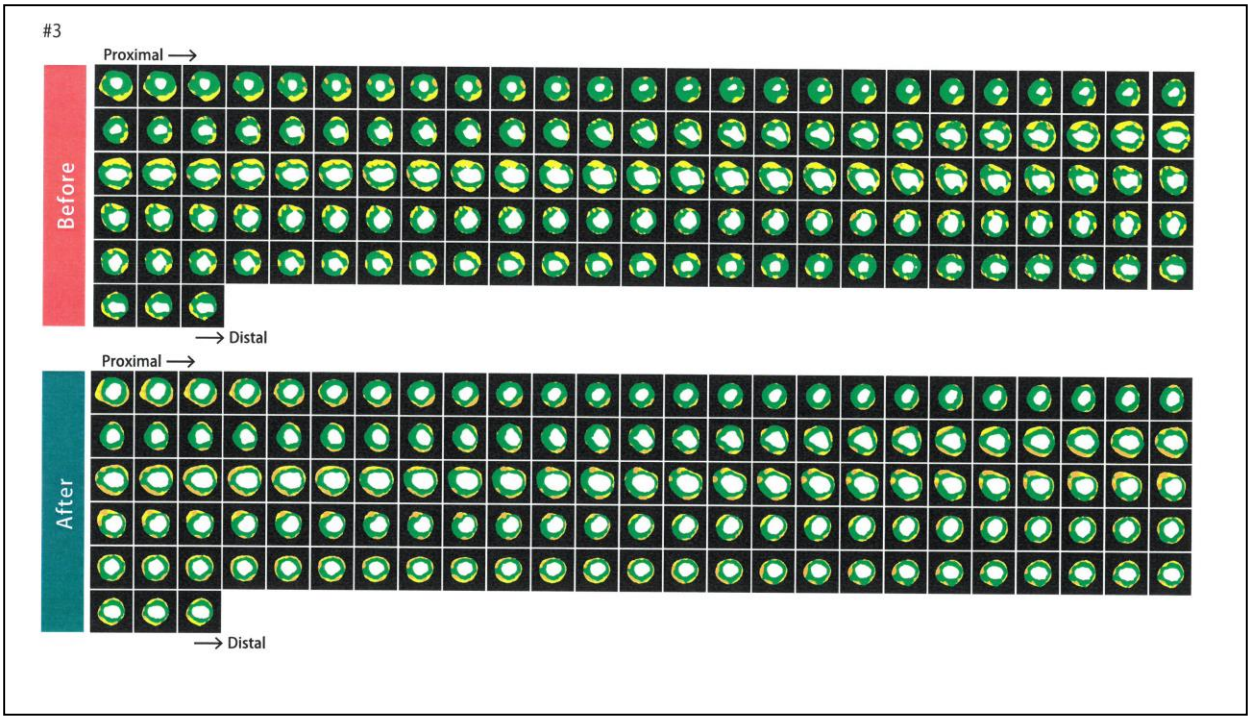

Fig. S2. Supplementary coronary CT images with a color-coded display in Case 2 (panel B)

The color-coded short-axis CT images before (upper panel) and after (on-treatment, lower panel) tricaprin treatment. The short-axis images of the right coronary anterior descending artery (Seg. #3) are shown every 0.2 mm.

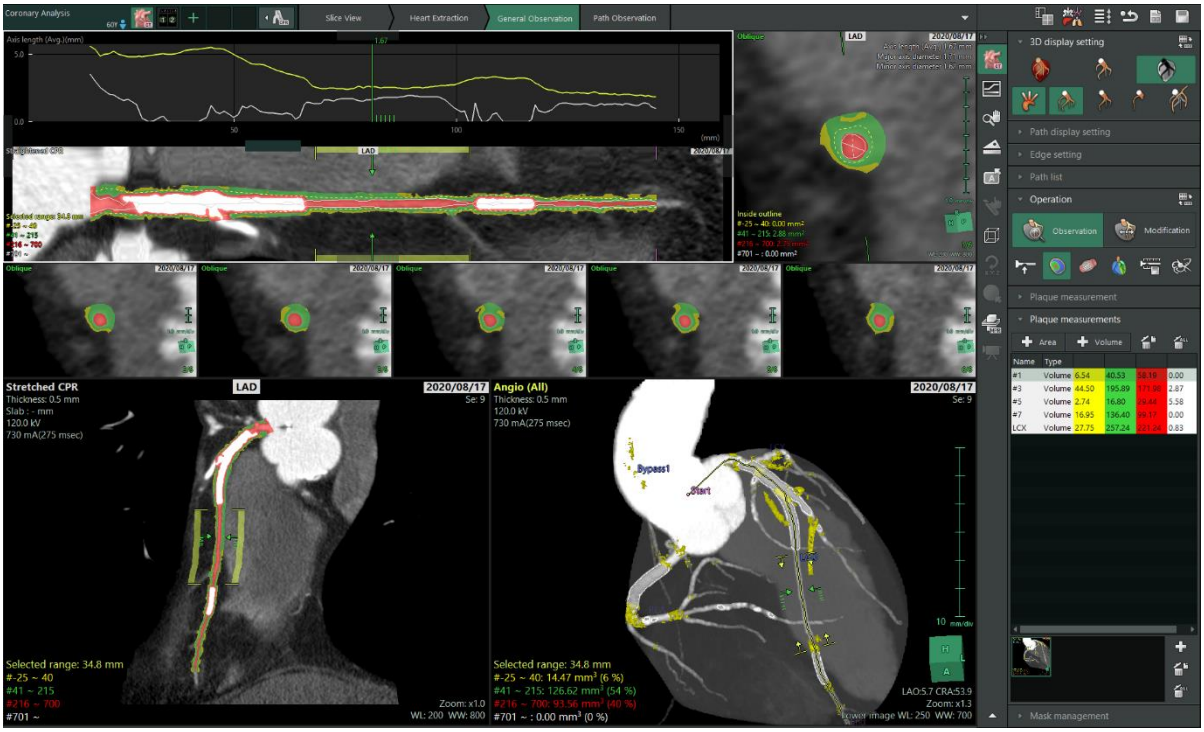

Fig. S3. Measurement of coronary artery wall volume and luminal volume in Case 2

The VINCENT (Fujifilm Medical Co., Ltd.) coronary artery analysis application was used.